Ain Shams Engineering Journal (2016) 7, 399–408

Ain Shams University

Ain Shams Engineering Journal

www.elsevier.com/locate/asej
www.sciencedirect.com

ELECTRICAL ENGINEERING

Unsteady MHD flow of an UCM fluid over a stretching surface with higher order chemical reaction

Sudhagar Palani, B. Rushi Kumar *, Peri K. Kameswaran

School of Advanced Sciences, VIT University, Vellore, TN, India

Received 18 June 2015; revised 12 October 2015; accepted 17 November 2015
Available online 4 February 2016

KEYWORDS

Unsteady flow;
Upper Converted Maxwell (UCM) fluid;
MHD flow;
Mass transfer;
Chemically reactive species;
Shooting method

Abstract The objective of this paper was to illustrate the frequent and wide occurrence of unsteady two dimensional MHD flow of an UCM fluid over a stretching surface in the presence of higher order chemical reaction in a diverse range of applications, both in nature and in technology. The governing partial differential equations are converted into ordinary differential equations by using similarity transformation. The ordinary differential equations were numerically solved by using shooting technique. The effects of different governing parameters on the flow field and mass transfer are shown in graphs and tables. The governing physical parameters significantly influence the flow field and mass transfer. Also, existing results in the literature are compared with the present study as a special case. In addition to practical applications in foams, suspensions, polymer solutions and melts, the present study also contributed to the existing literature.

1. Introduction

The boundary layer flows of non-Newtonian fluid have received much importance due to its numerous industrial and engineering applications. In view of non-Newtonian fluids diverse rheological properties cannot be examined through one constitutive relationship between shear stress and rate of strain. For any boundary layer, Maxwell model is used to predict stress relaxation and also excludes the effects of shear dependent viscosity. Sakiadis [1] first investigated the boundary layer flow of a viscous fluid, and the flow is caused due to the motion of the rigid plane sheet in its own plane. Due to entrainment to ambient fluid, this situation represents a different class of boundary-layer problem which has a solution substantially different from that of boundary-layer flow over a semi-infinite flat plate. Erickson et al. [2] extended this problem to the moving surface in the presence of suction or blowing. Crane [3] considered the moving sheet, and the velocity is proportional to the distance from the slit. In general, these types of flows occur in the drawing of plastic films and artificial fibers. Gupta and Gupta [4] investigated heat and mass transfer over a stretching sheet with suction or blowing. Similarity solution of MHD boundary layer flow problem of an electrically conducting incompressible fluid over a stretching surface

* Corresponding author. Tel.: +91 9566927966.
E-mail address: rushikumar@vit.ac.in (B. Rushi Kumar).
Peer review under responsibility of Ain Shams University.

Production and hosting by Elsevier

http://dx.doi.org/10.1016/j.asej.2015.11.021
2090-4479 © 2016 Faculty of Engineering, Ain Shams University. Production and hosting by Elsevier B.V.

in the presence of transverse magnetic field was studied by pavlov [5]. Chakrabarti and Guptav [6] extended the problem to the temperature distribution in the MHD boundary layer flow due to stretching surface with suction.

Non-Newtonian fluids with convective heat and mass transfer finds many industrial applications such as nuclear fuel slurries, paper coating, liquid metals, movement in biological fluids, plastic extrusion, material processing and crystal growing. The behavior of non-Newtonian fluid has been characterized by upper-convected Maxwell model. The Rayleigh-Stokes problem and the Maxwell fluid flow past an infinite plate were investigated by Fatecau and Fatecau [7,8]. Sadeghy and Sharifi [9] presented a comparative analysis for Sakiadis flow of an Upper-Convected Maxwell (UCM) fluid on a fixed plate and concluded that the Deborah number increases with decrease in skin friction at the wall. Mass transfer phenomenon is the movement of mass from one region to another region in the system. This physical process is applied in several scientific fields such as variable systems and chemical change that affect molecular and convective diffusion of atoms and molecules. The driving force for movement of mass is a difference in concentration, and the random motion of molecules causes a net movement of mass from a high concentration region to the low concentration region. Liu [10] and Cortell [11] investigated the heat and mass transfer in the presence of the hydromagnetic flow over a stretching surface. Momentum and mass transfer characteristics of chemical reactive species with first and higher order reactions for electrically conducting viscoelastic fluid are influenced by a porous stretching sheet. Andersson et al. [12] discussed the momentum and mass diffusion of the flow with chemical reactive species over a stretching sheet. Takhar et al. [13] presented the mass transfer with magnetohydrodynamic (MHD) flow in a viscous electrically conducting fluid by a stretching sheet with nonzero velocity. The problem of second grade fluid with a porous medium was extended by Akyildiz et al. [14]. The effects of suction/blowing with heat absorption/generation over a porous stretching surface in the presence of boundary layer flow were analyzed by Layek et al. [15]. Hayat et al. [16] studied the magnetohydrodynamic boundary layer flow of a Jeffery fluid bounded by a stretching sheet and solved the governing equations by using homotopy analysis method. Different analytical techniques such as LSM, DTM, OHAM, and HPM, were studied by Ghasemi et al. [19,20], Vatani et al. [21] and Mohammadian et al. [22].

The effects of combined heat and mass transfer of third grade nanofluids over a convectively heated stretching permeable surface were studied by Khan et al. [23]. Their study is based on Buongiorno model for the nanofluids. Various boundary layer flow problems on past a stretching sheet and vertical porous plate were studied by Makinde [24], Makinde and Sibanda [25], Makinde and Olanrewaju [26] and Anver Beg and Makinde [27].

In this paper our aim was to investigate unsteady boundary layer MHD flow and mass transfer of an UCM fluid in the presence of higher order chemical reaction. The rest of this paper is organized as follows: Section 2 is devoted to the mathematical formulation of the problem. Section 3 deals with the exact solutions in certain cases. In Section 4, the numerical solution of the problem is introduced. Section 5 deals with the results and discussion. Section 6 gives the conclusion.

2. Mathematical formulation

2.1. Transient unsteady-state flow and mass transfer ($t > 0$)

We consider the unsteady and incompressible MHD flow and mass transfer of an electrically conducting upper convected Maxwell fluid over a stretching surface. The flow is induced due to the stretching surface by applying equal and opposite forces by the x-axis and considering the flow to be bounded to the region $y > 0$. The mass flow and unsteady fluid start at $t = 0$. The sheet appears out of a slit at origin and moves with velocity $U(x,t) = \frac{bx}{1-\alpha t}$ where b and α are positive constants both having dimensions $(time)^{-1}$, b is the rate of stretching and $\frac{b}{1-\alpha t}$ is the rate of stretching with time. In case of polymer, the material properties of the sheet vary with time. A uniform magnetic field of strength B_0 is along the y-axis. The induced magnetic field is trifling, which is a valid assumption on a scale under the small magnetic Reynolds number and the external field is zero. The problem of mass transfer in the flow along a flat plate that contains a species, say A is slightly soluble in B. C_w be the concentration at the plate surface and C_∞ be the solubility of A in B and in the concentration of species far away from the plate is A. Let the rate of reaction of the species A with B be an nth-order homogenous chemical reaction with constant k_n. The flow geometry and coordinate system is shown in Fig. 1.

It is desirable to study the system by the boundary layer analysis [17]. The governing equations of the model [18] are expressed as

$$\frac{\partial u}{\partial x} + \frac{\partial v}{\partial y} = 0, \tag{1}$$

$$\frac{\partial u}{\partial t} + u\frac{\partial u}{\partial x} + v\frac{\partial u}{\partial y} + \lambda\left(u^2\frac{\partial^2 u}{\partial x^2} + v^2\frac{\partial^2 u}{\partial y^2} + 2uv\frac{\partial^2 u}{\partial x \partial y}\right) = v\frac{\partial^2 u}{\partial y^2} - \frac{\sigma B_0^2}{\rho}u, \tag{2}$$

$$\frac{\partial C}{\partial t} + u\frac{\partial C}{\partial x} + v\frac{\partial C}{\partial y} = D\frac{\partial^2 C}{\partial y^2} - K_n(C - C_\infty)^n, \tag{3}$$

The initial conditions are as follows:

$$u(x,0) = u(x), \quad v(x,0) = -v_0, \quad C(x,0) = C_w(x), \tag{4}$$

The appropriate boundary conditions for Eqs. (1)–(3) have the form:

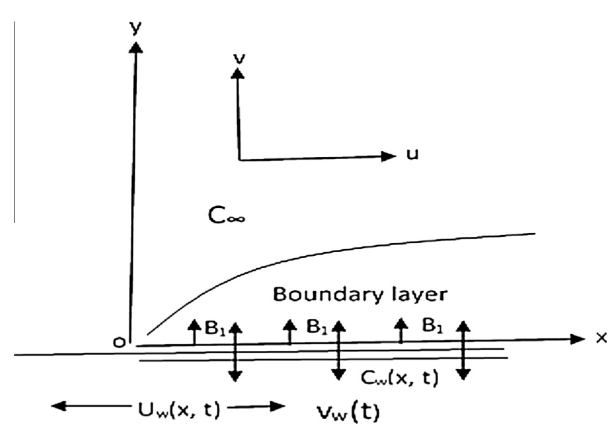

Figure 1 Flow model and physical coordinate system.

$$u(x,t) = U_w(x,t) = \frac{bx}{1-\alpha t}, \quad v(x,t) = v_w(t),$$
$$C(x,t) = C_w(x,t) \quad \text{at} \quad y = 0,$$
$$u(x,t) \to 0, \quad C(x,t) \to C_\infty \quad \text{as} \quad y \to \infty, \tag{5}$$

Here, u and v are the components of velocity in x and y directions respectively, λ is the relaxation time, v is the fluid kinematic viscosity, σ is the fluid conductivity, B_0 is the uniform magnetic field, ρ is the density of fluid, C is the species concentration, D is the coefficient of diffusion in the diffusing species of the fluid and K_n is the rate of reaction constant of order n. Where the surface concentration of the sheet is assumed to vary by both the sheet and time, in accordance with $C_w(x,t) = C_\infty + bx(1-\alpha t)^{-2}$. The wall concentration $C_w(x,t)$ increases (reduces), if b is positive (negative) and is in proportion to x. Moreover, the amount of concentration increase (reduce) along the sheet increases with time. Here $v_w(t) = -\frac{v_0}{\sqrt{1-\alpha t}}$ is the velocity of suction $v_0 > 0$ or blowing $v_0 < 0$. The expression for $U_w(x,t), v_w(t), C_w(x,t)\ \lambda(t), K_n(t)$ is valid for time $t < \alpha^{-1}$.

Continuity Eq. (1) is satisfied by introducing a stream function $\psi(x,y,t)$ such that

$$u = \frac{\partial\psi}{\partial y} \quad \text{and} \quad v = -\frac{\partial\psi}{\partial x},$$

where $\psi = \sqrt{\frac{vb}{1-\alpha t}}\, xf(\eta)$ and $\eta = \sqrt{\frac{b}{1-\alpha t}}\, y$, are the dimensionless stream function and similarity variable, respectively.

The velocity components are given by

$$u = \frac{bx}{(1-\alpha t)} f'(\eta) \quad \text{and} \quad v = -\sqrt{\frac{vb}{1-\alpha t}}\, f(\eta) \tag{6}$$

The concentration is represented as

$$\phi(\eta) = \frac{C - C_\infty}{C_w - C_\infty} \quad \text{and} \quad C = C_\infty + bx(1-\alpha t)^{-2}\phi(\eta) \tag{7}$$

Using Eqs. (4)–(7), Eqs. (2) and (3) transform the following boundary value problems

$$M\left(\frac{\eta}{2}f'' + f'\right) + f'^2 - ff'' + \beta\left(f^2 f''' - 2ff'f''\right) = f''' - Haf', \tag{8}$$
$$M\left(2\phi + \frac{\eta}{2}\right) + f'\phi - f\phi' = \frac{1}{Sc}\phi'' - \gamma\phi^n, \tag{9}$$
$$f(0) = S, \quad f'(0) = 1, \quad f'(\infty) \to 0, \tag{10}$$
$$\phi(0) = 1, \quad \phi(\infty) \to 0. \tag{11}$$

where a prime refers to differentiation with respect to η. The dimensionless parameters in Eqs. (8)–(10) are the unsteadiness parameter M, the Maxwell parameter β, the Magnetic parameter Ha, the Schmidt number Sc, the reaction rate parameter γ and the suction/blowing parameter S, which can be represented as follows

$$M = \frac{\alpha}{b}, \quad \beta = \lambda_0 b, \quad Ha = \frac{\sigma B_0^2}{\rho b}(1-\alpha t), \quad Sc = \frac{v}{D},$$
$$\gamma = \frac{K_n (C_w - C_\infty)^{n-1}}{b}, \quad S = -\frac{v_0}{\sqrt{vb}}$$

It is worth mentioning that the chemical reaction parameter γ is a real number, $\gamma < 0$ indicates the destructive chemical reaction, $\gamma > 0$ denotes the generative chemical reaction, and $\gamma = 0$ for the non-reactive species. It follows that for suction S is positive and S is negative for blowing, and this parameter is used to controlling the normal flow strength and direction at the boundary.

2.2. Skin friction, Mass transfer coefficients

For practical purposes, the functions $f(\eta)$ and $\phi(\eta)$ allow us to determine the skin friction coefficient and mass transfer rates.

The shearing stress at the surface of the wall τ_w is given by

$$\tau_w = \mu\left[\frac{\partial u}{\partial y}\right]_{y=0} \tag{12}$$

where μ is the coefficient of viscosity. The skin friction coefficient is defined as

$$C_f = \frac{\tau_w}{\rho U_w^2} \tag{13}$$

and using Eq. (12) in Eq. (13), we obtain

$$C_f\sqrt{Re_x} = f''(0), \tag{14}$$

The mass flux at the surface of the wall is given by

$$J_w = D\left[\frac{\partial C}{\partial y}\right]_{y=0} \tag{15}$$

and the Sherwood is defined as

$$Sh_x = \frac{x}{D}\frac{J_w}{C_w - C_\infty}. \tag{16}$$

Using (15) in (16) the dimensionless wall mass transfer rate is obtained as

$$\frac{Sh_x}{\sqrt{Re_x}} = \phi'(0). \tag{17}$$

where

$$Re_x = \frac{U_w x}{v}$$

is the local Reynolds number.

3. Exact solutions for some special cases

3.1. Initial steady state flow and mass transfer ($t \le 0$)

In case of steady state solution i.e., $M \to 0$, Eqs. (8) and (9) along with the boundary conditions (10) and (11) are replaced by

$$f''' = f'^2 - ff'' + \beta\left(f^2 f''' - 2ff'f''\right) + Haf', \tag{18}$$
$$\phi'' = Sc(f'\phi - f\phi' + \gamma\phi^n), \tag{19}$$
$$f(0) = S, \quad f'(0) = 1, \quad f'(\infty) \to 0, \tag{20}$$
$$\phi(0) = 1, \quad \phi(\infty) \to 0. \tag{21}$$

Here we presented the solution of momentum and mass transfer equation, when $\beta = Ha = 0$ and $n = 1$ as particular case, then Eqs. (18) and (19) are replaced by

$$f''' = f'^2 - ff'', \tag{22}$$
$$\phi'' = Sc(f'\phi - f\phi' + \gamma\phi). \tag{23}$$

3.2. Solution of momentum equation

The momentum boundary layer equation is partially decoupled from the species equations. The solution is obtained by

Table 1 Comparison of $f''(0)$ for different values Ha in the absence of the parameters $\beta = S = \gamma = Sc = 0, n = 1$.

Results	$Ha = 0$	$Ha = 0.5$	$Ha = 1$	$Ha = 1.5$	$Ha = 2$
Present results	−1.000000	−1.224745	−1.414214	−1.581139	−1.732051
Anderson et al. [12]	−1.000000	−1.224900	−1.414000	−1.581000	−1.732000
Prasad et al. [29]	−1.000174	−1.224753	−1.414449	−1.581139	−1.732203
Mukhopadhyay et al. [30]	−1.000173	−1.224753	−1.414450	−1.581140	−1.732203

Table 2 Comparison of $f''(0)$ for different values of M, when $\beta = Ha = S = \gamma = Sc = 0, n = 1$.

Results	Sharidan et al. [31]	Chamkha et al. [32]	Bhattacharyya et al. [33]	Present study
$M = 0.8$	−1.261042	−1.261512	−1.261487	−1.261043
$M = 1.2$	−1.377722	−1.378052	−1.377910	−1.377724

looking for an exponential function of the form $f'(\eta) = e^{-s\eta}$ that satisfies both the differential equation and governing boundary conditions over the interval $[0, \infty)$, and an exact solution to Eqs. (22) and (20) is obtained as

$$f(\eta) = \frac{1 - e^{-s\eta}}{s}, \tag{24}$$

where s is the parameter defined as follows

$$s = 1. \tag{25}$$

was shown by Crane [3].

3.3. Solution of the mass transport equation

Introducing a new variable

$$\xi = -\frac{Sc}{s^2} e^{-s\eta}, \tag{26}$$

Eq. (23) and the boundary conditions in (21) take the form:

$$\xi \phi_{\xi\xi} + (1 - Sc^* - \xi)\phi_\xi + \left(1 - \frac{1}{\xi}\gamma Sc^*\right)\phi = 0, \tag{27}$$

$$\phi(-Sc^*) = 1, \quad \phi(0^-) \to 0. \tag{28}$$

where $Sc^* = Sc/s^2$ is the modified Schmidt number. The solution of Eq. (27) is obtained in terms of confluent hypergeometric functions in the following form

$$\phi(\xi) = a_0\, \xi^{\frac{a+b}{2}}\, K\left[\frac{a+b}{2} - 1,\ 1 + b,\ \xi\right], \tag{29}$$

where

$$K[a,\ b,\ z] = \sum_{r=0}^{\infty} \frac{a(a+1)\ldots(a+r-1)}{b(b+1)\ldots(b+r-1)} \frac{z}{r!}$$

is Kummer's function making use of the boundary conditions (28) and rewriting the solution in terms of the variable η, we get

$$\phi(\eta) = \frac{e^{-\left(\frac{a+b}{2}\right)s\eta}\, K\left[\frac{a+b}{2} - 1,\ 1 + b,\ -Sc^* e^{-s\eta}\right]}{K\left[\frac{a+b}{2} - 1,\ 1 + b,\ -Sc^*\right]}, \tag{30}$$

where

$$a = Sc^*, \quad b = \sqrt{(Sc^*)^2 + 4\gamma Sc^*}.$$

4. Numerical solution of the problem

Governing Eqs. (8) and (9) subject to conditions (10) and (11) are solved numerically using Runge–Kutta fourth order method along with shooting technique. The higher order non-linear partial differential equations are converted into first order simultaneous linear differential equations and then transformed to initial value problem (Jain et al. [28]). In this method the third-order nonlinear Eq. (8) and second order

Table 3 Comparison of $f''(0), \phi'(0)$ for different values of the parameters, when $M = Sc = 1, \gamma = 0$.

Ha	β	$f''(0)$			$\phi'(0)$		
		$S = -0.1$	$S = 0.0$	$S = 0.5$	$S = -0.1$	$S = 0.0$	$S = 0.5$
0.0	0.0	−1.27796	−1.32336	−1.57817	−1.63427	−1.68113	−1.93695
	0.2	−1.29551	−1.35881	−1.79027	−1.63189	−1.67745	−1.92169
	0.4	−1.31268	−1.39409	−2.03301	−1.62957	−1.67385	−1.90559
	0.6	−1.32945	−1.42912	−0.86584	−1.62730	−1.67032	−0.43760
	0.8	−1.34581	−1.46383	−0.86584	−1.62509	−1.66687	−0.43760
0.5	0.0	−1.45317	−1.49947	−1.75574	−1.62107	−1.66792	−1.92425
	0.2	−1.46727	−1.53142	−1.96690	−1.61913	−1.66474	−1.90992
	0.4	−1.48104	−1.56318	−2.20736	−1.61722	−1.66163	−1.89489
	0.6	−1.49449	−1.59471	−0.96482	−1.61536	−1.65858	−0.34935
	0.8	−1.50762	−1.62597	−0.96482	−1.61354	−1.65561	−0.34935
1.0	0.0	−1.61068	−1.65757	−1.91458	−1.60988	−1.65672	−1.91352
	0.2	−1.62211	−1.68679	−2.12541	−1.60826	−1.65394	−1.89998
	0.4	−1.63330	−1.71583	−2.36474	−1.60667	−1.65121	−1.88581
	0.6	−1.64422	−1.74468	−0.76804	−1.60511	−1.64854	−0.28618
	0.8	−1.65489	−1.77331	−0.76804	−1.60359	−1.64592	−0.28618

Table 4 Concentration gradient $\phi'(0)$ for different physical parameters, when $M = 1$.

Sc	S	γ	β	$f''(0)$			$\phi'(0)$		
				$n=1$	$n=2$	$n=3$	$n=1$	$n=2$	$n=3$
1.0	− 0.1	−0.2	0.0	−1.56979	−1.59223	−1.60305	−1.55572	−1.57848	−1.58947
			0.2	−1.56723	−1.58974	−1.60060	−1.55363	−1.57644	−1.58746
		0.5	0.0	−1.78407	−1.73465	−1.70973	−1.77261	−1.72264	−1.69739
			0.2	−1.78205	−1.73251	−1.70751	−1.77095	−1.72088	−1.69558
	0.0	−0.2	0.0	−1.61642	−1.63943	−1.65033	−1.60233	−1.62567	−1.63674
			0.2	−1.61248	−1.63559	−1.64654	−1.59893	−1.62235	−1.63347
		0.5	0.2	−1.83136	−1.78080	−1.75567	−1.81989	−1.76876	−1.74329
			0.2	−1.82821	−1.77747	−1.75223	−1.81716	−1.76587	−1.74032
	0.5	−0.2	0.0	−1.87204	−1.63943	−1.90842	−1.85848	−1.62567	−1.89542
			0.2	−1.85577	−1.88156	−1.89280	−1.85848	−1.86937	−1.88075
		0.5	0.0	−2.08745	−2.03202	−2.00633	−2.07641	−2.02032	−1.99431
			0.2	−2.07416	−2.01796	−1.99188	−2.06391	−2.00712	−1.98075
β	S	γ	Sc	$n=1$	$n=2$	$n=3$	$n=1$	$n=2$	$n=3$
0.2	− 0.1	−0.2	1	−1.56723	−1.58974	−1.6006	−1.55363	−1.57644	−1.58746
			2	−2.23271	−2.26308	−2.27786	−2.217	−2.24777	−2.26274
			3	−1.78586	−1.63186	−1.74262	−1.58055	−1.23061	−1.31741
		0.5	1	−1.78205	−1.73251	−1.70751	−1.77095	−1.72088	−1.69558
			2	−2.5278	−2.46027	−2.42609	−2.5151	−2.44689	−2.41233
			3	−1.02192	−1.62655	−2.42609	−0.877197	−1.45179	−1.28696
	0.0	−0.2	1	−1.61248	−1.63559	−1.64654	−1.59893	−1.62235	−1.63347
			2	−2.32749	−2.35886	−2.37377	−2.31169	−2.34349	−2.3586
			3	−2.33409	−2.20616	−2.33046	−2.10651	−1.95426	−2.1723
		0.5	1	−1.82821	−1.77747	−1.75223	−1.81716	−1.76587	−1.74032
			2	−2.62349	−2.55387	−2.51931	−2.61074	−2.54039	−2.50545
			3	−1.63546	−2.31034	−2.51931	−1.41203	−1.94468	−2.50545
	0.5	−0.2	1	−1.85577	−1.88156	−1.8928	−1.84323	−1.86937	−1.88075
			2	−2.85864	−2.89383	−2.90884	−2.84359	−2.87927	−2.89446
			3	−3.71013	−3.75234	−3.77009	−3.69397	−3.73673	−3.75466
		0.5	1	−2.07416	−2.01796	−1.99188	−2.06391	−2.00712	−1.98075
			2	−3.15274	−3.07481	−3.03961	−3.14054	−3.06178	−3.02621
			3	−4.05934	−3.96503	−3.92316	−4.04624	−3.95096	−3.9087

Table 5 Comparison of the values of wall mass transfer rates $\phi'(0)$ for different values of chemical reaction parameters, when $M = \beta = Ha = S = 0, n = 1, Sc = 5$.

Results	$\gamma = -0.2$	$\gamma = -0.1$	$\gamma = 0$	$\gamma = 0.1$	$\gamma = 0.2$
Analytical	−2.342239	−2.452574	−2.557600	−2.658032	−2.754441
Numerical	−2.342239	−2.452574	−2.557600	−2.658032	−2.754441

Eq. (9) have been reduced to ordinary differential equations as follows:

$$f_1' = f_2, \quad f_2' = f_3$$

$$f_3' = \frac{M\left(\frac{\eta}{2}f_3 + f_2\right) + f_2^2 - f_1 f_3 - 2\beta f_1 f_2 f_3 + Ha f_2}{1 - \beta f_1^2}$$

$$f_4' = f_5$$

$$f_5' = Sc\left[M\left(2f_4 + \frac{\eta}{2}\right) + f_2 f_4 - f_1 f_5 + \gamma f_4^n\right] \tag{31}$$

where

$$f_1 = f, \quad f_2 = f', \quad f_3 = f'', \quad f_4 = \phi, \quad f_5 = \phi', \tag{32}$$

and a prime denotes differentiation with respect to η. The boundary conditions now become

$$f_1 = S, \ f_2 = 1, \ f_3 = s_1, \ f_4 = 1, \ f_5 = s_2, \ \text{at} \ \eta \to 0 \tag{33}$$

$$f_2 = 0, \ f_4 = 0, \ \text{as} \ \eta \to \infty, \tag{34}$$

5. Result and discussion

To assess the accuracy of the present method, the results of skin friction coefficient $f''(0)$ for the steady motion in the absence of suction/blowing with $n = 1$ are compared with the available results shown in Table 1.

Moreover, the present results for the skin friction coefficient $f''(0)$ for an unsteady motion of the Newtonian fluid ($\beta = 0$) are compared with the available results of Sharidan et al. [31], Chamakha et al. [32] and Bhattacharyya et al. [33] in Table 2 and the results are also in good agreement with each other.

Furthermore, the values of $f''(0)$ and $\phi'(0)$ are given in Tables 3 and 4 for various values of the physical parameters, namely $M, S, \beta, \gamma, Sc, n$ and Ha. From these tables, we noticed that $f''(0)$ decreases with the increases in Maxwell parameter, magnetic parameter, and injection parameter, whereas the

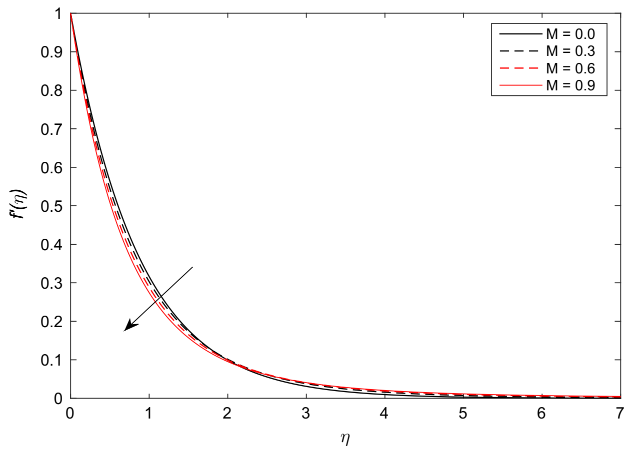

Figure 2 Velocity profiles for different values of M with similarity variable η for $\beta = Ha = S = 0.1$.

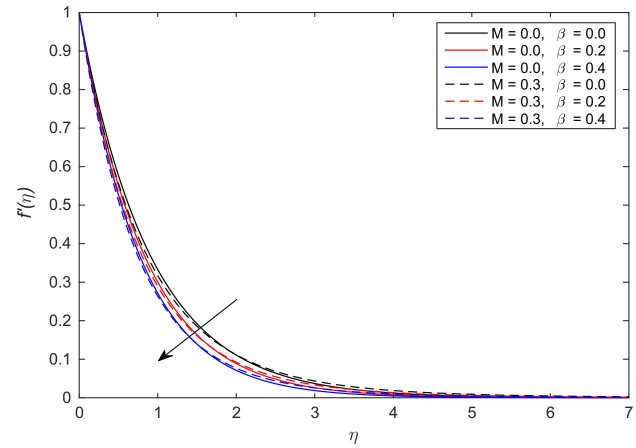

Figure 4 Velocity profiles for various values of β for the steady and unsteady motion when $Ha = S = 0.1$.

reverse trend is found with mass diffusion parameter. It is to note that the magnitude of the wall concentration gradient increases with Sc and γ. It is further noted that the effect of a higher-order chemical reaction is to enhance the concentration gradient for destructive chemical reaction. However, the opposite trend is observed with generative chemical reaction.

Table 5 provides the values of the mass transfer coefficient $\phi'(0)$ for the various values of the γ. It is noticed that mass transfer rate is enhanced from destructive chemical reactions to constructive chemical reaction. Moreover, it can also be observed that good agreement is found between analytical and numerical results.

The numerical calculations are carried out for different values of the physical parameters involved in equations: unsteadiness parameter M, Maxwell parameter β, Magnetic parameter Ha, chemical reaction parameter γ, order of chemical reaction n and suction/blowing parameter S. In order to analyze salient features of the problem, the numerical results are shown in figures and physical explanations are discussed for all cases. Fig. 2 shows the velocity profiles for various values of unsteadiness parameter M. It is noted that the velocity along the sheet decreases as the boundary layer thickness decreases near the wall; however, the velocity of fluid increases away from the wall with the increase of M.

In Fig. 3 exhibits the effects of M for the concentration species. From these figures, it is seen that at a particular point the concentration profile decreases as M increases. Also there is a decrease in the mass transfer rate form fluid to sheet when M increases. Hence, the concentration $\phi(\eta)$ decreases.

Since the flow is entirely induced by the stretching surface concentration and it is higher than stream concentration, both the velocity and concentration decrease with increasing η. The wall concentration gradient is positive i.e., there is a mass diffusion from the fluid to the surface. The increase in concentration profiles is observed near the sheet. By comparing the figures with that for a higher-order chemical reaction are exhibited in Fig. 3(b) and (c). The effects of β on the velocity profiles for steady and unsteady motion are shown in Fig. 4. It is noticed that the results of velocity profiles are similar for large values of β and become larger in the case of suction. As β increases the thickness of the boundary layer decreases.

The effect of increase in the Maxwell parameter causes the enhancement of the concentration profiles ϕ across the flow in

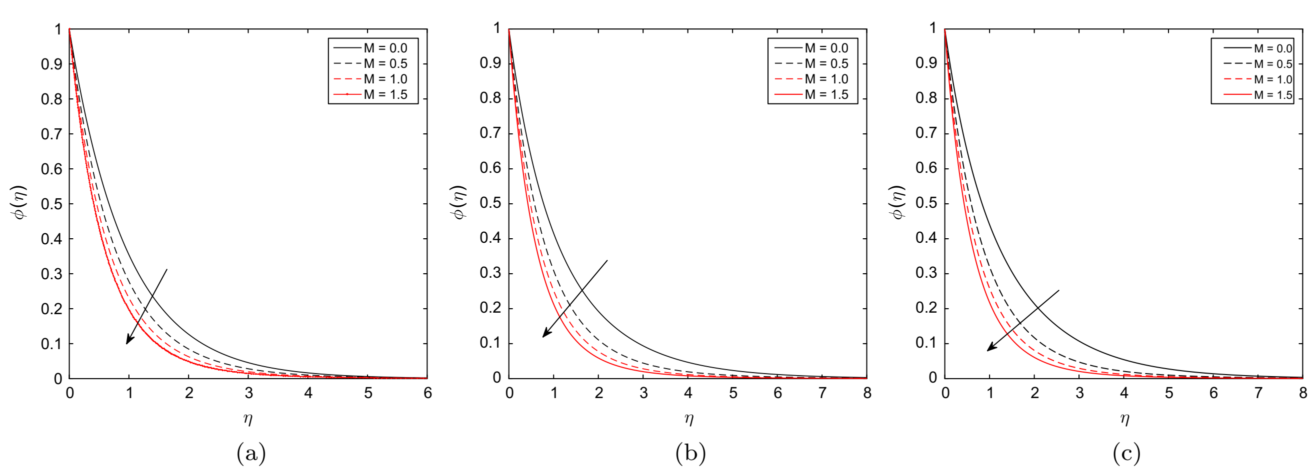

Figure 3 Concentration profiles for different values of M with similarity variable η for (a) $n = 1$ (b) $n = 2$ and (c) $n = 3$, when $\beta = Ha = S = 0.1, \gamma = 0.5, Sc = 0.7$.

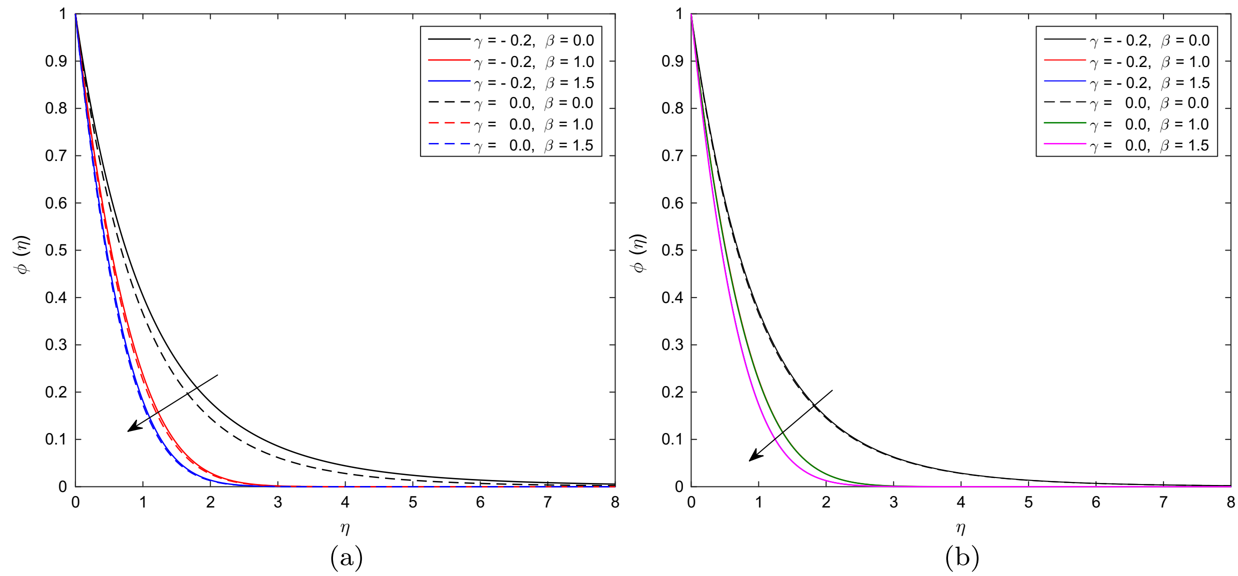

Figure 5 Concentration profiles for different values of γ and β with similarity variable η for (a) $n = 1$ and (b) $n = 3$, when $M = 0.3, Ha = S = 0.1, Sc = 0.7$.

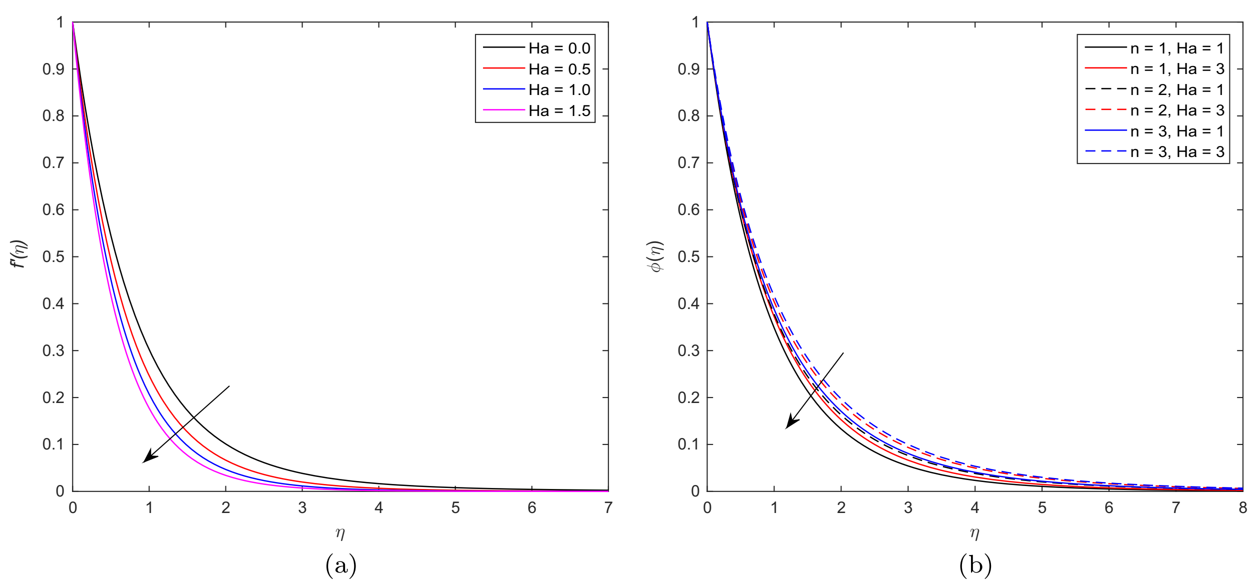

Figure 6 (a) Velocity for different values of Ha with similarity variable η for $M = 0.3, \beta = 0.2, S = 0.1$ and (b) Concentration profiles for various values of n and Ha with similarity variable η for $M = \gamma = 0.3, \beta = 0.2, S = 0.1, Sc = 0.7$.

the unsteady motion for $n = 1$ and $n = 3$ respectively which is shown in Fig. 5(a) and (b). The rate of mass diffusion at the surface increases with the increase of Maxwell parameter as shown in figures. It shows the effect of β on the concentration field ϕ for a non-reactive species $\gamma = 0$, destructive chemical reactions $\gamma > 0$ and generative chemical reactions $\gamma < 0$ respectively. It is observed from these figures that ϕ decreases for large values of β in case of generative chemical reaction ($\gamma < 0$). But the magnitude of ϕ is greater ($\gamma < 0$) when compared with the case of destructive chemical reaction ($\gamma > 0$).

It is also observed that the effect of increasing β in all cases ($\gamma = 0, \gamma < 0, \gamma > 0$) decreases the concentration field ϕ. The effects of increasing magnetic parameter Ha on both velocity and concentration profiles for the first, second and third order chemical reactions are shown in Fig. 6(a) and (b). The velocity of the fluid decreases with the increase of magnetic field in Fig. 6(a). Physically, this fact is well known an electrical conducting fluid exposed across a magnetic field will give rise to body force known as Lorenz force. The concentration of the fluid increases with increase in the fluid resistance by increasing the friction between its layers. This trend holds good for non-linear (higher-order) chemical reaction, as shown in Fig. 6(b). Comparison to the figures exposes the effect of increasing the order of the chemical reaction n is to enhance the wall

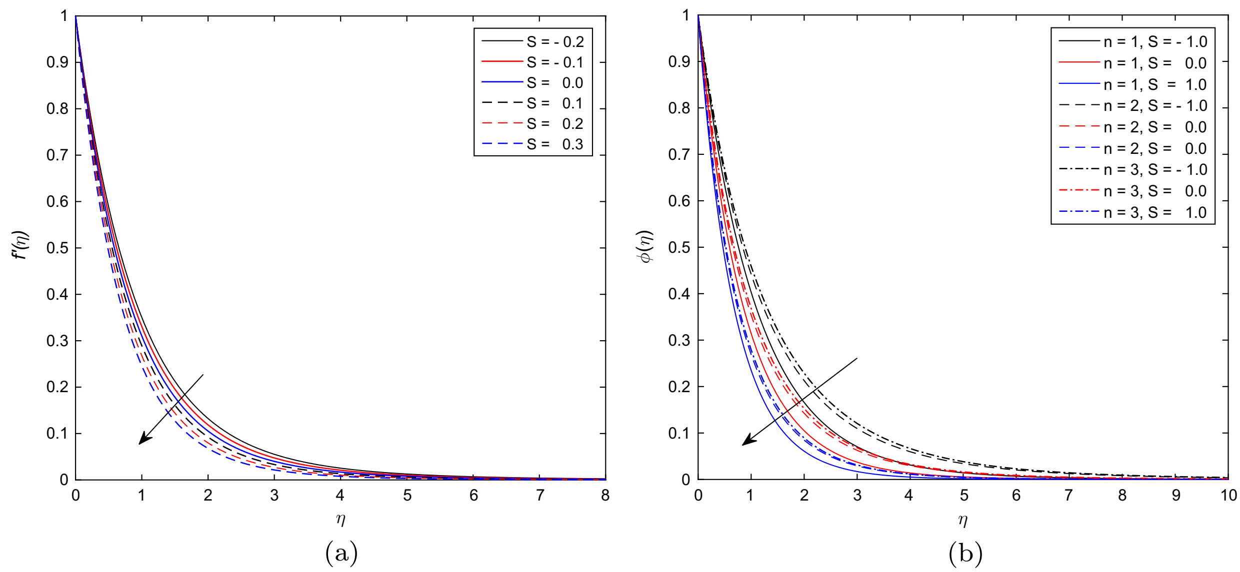

Figure 7 Velocity for different values of S with similarity variable η for $M = 0.3, \beta = 0.2, Ha = 0.1$ and (b) Concentration profiles for various values of n and S with similarity variable η for $M = 0.3, \gamma = 0.5, \beta = 0.2, Sc = 0.7$.

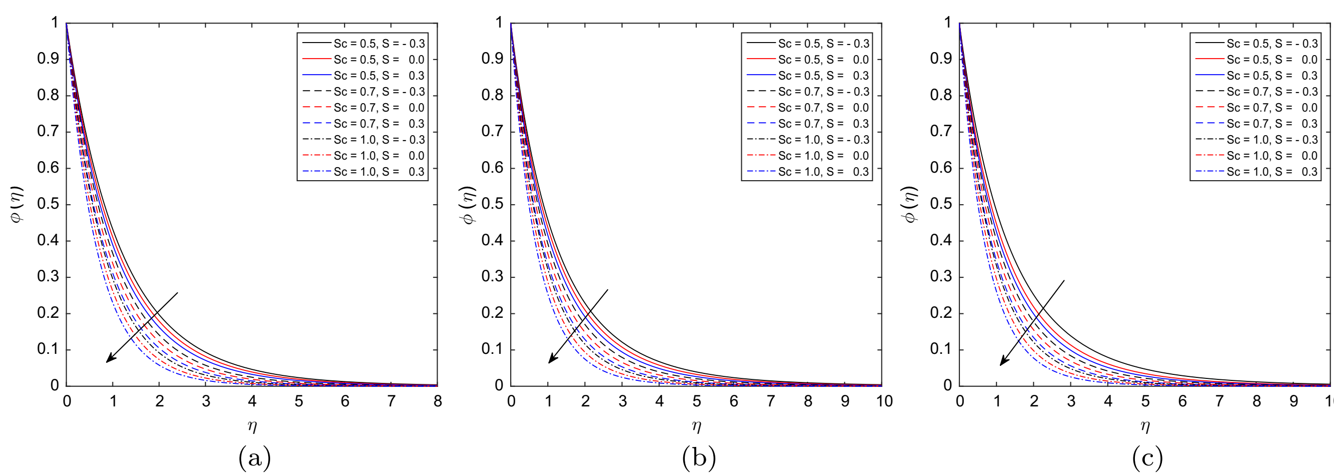

Figure 8 Concentration profiles for different values of Sc and S with similarity variable η for (a) $n = 1$ (b) $n = 2$ and (c) $n = 3$, when $\beta = 0.2, Ha = 0.1, M = \gamma = 0.3$.

concentration gradient shown in Table 3. Hence the thickness of the species distribution increases as n increases.

Fig. 7(a) gives the variations of S on the velocity f'. It is observed decrease in the magnitude of the velocity when S increases. The shrinking sheet is not confined inside a boundary layer and the flow is different when suction on the boundary is imposed. Thus suction appears when the fluid changes on the surface. Physically, in case of shrinking sheet, suction plays very important role in helping the fluid flow smoothly. With S increases the thickness of the boundary layer decreases. Fig. 7(b) gives the variations of S on the concentration field ϕ. It is found that the concentration field decreases as the value of suction/blowing parameter S increases ($S > 0$). This effects a decrease in mass transfer rate. It is quit opposite in the case of blowing ($S < 0$). The thickness of the boundary layer is thinner in the case of suction ($S > 0$) than in the case of impermeability ($S = 0$) when it is thicker in the case of blowing ($S < 0$).

Fig. 8(a) to (c) depicts the concentration profiles respectively for the first, second and third order chemical reactions for variable values of Schmidt number Sc. It is observed that the increasing values of Schmidt number extends to a decrease in the concentration boundary layer thickness. This is caused by the thinning of the concentration boundary layer with the species diffusion (D) and the Schmidt number is inversely proportional to the diffusion coefficient. This effect is higher in case of suction ($S > 0$) than in the cases of impermeability ($S = 0$) and blowing ($S < 0$).

From Fig. 9, the concentration profiles ϕ are plotted for the different values of the reaction-rate parameter γ, when the other parameters are fixed. Concentration increases as reaction rate parameter γ increases. This result is true in the cases of destructive chemical reaction $\gamma > 0$ and generative chemical reaction $\gamma < 0$. By comparing the figure with that for a higher-order chemical reaction, we notice that the thickness of concentration boundary layer is higher for a third order

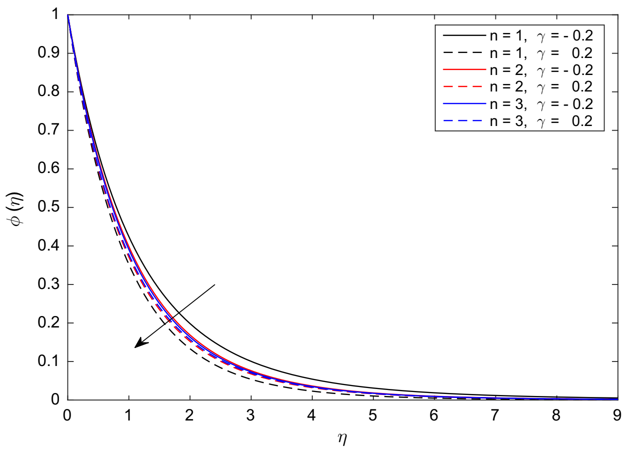

Figure 9 Concentration profiles for various values of higher order chemical reaction and γ with similarity variable η for $M = 0.3, \beta = 0.2, S = 0, Ha = 0.1, Sc = 0.7$.

chemical reaction as compared to the first or second-order chemical reaction.

6. Conclusions

In this work, unsteady boundary layer MHD flow of a Maxwell fluid over a stretching surface in the presence of higher order constructive/destructive chemical reaction is obtained. Qualitative explanation for UCM fluid behavior is to provide some insights into the nature of underlying physical processes. The following observations have been made:

- For increasing values of M the velocity of the fluid decreases initially and increases at the end. The concentration of fluid also decreases significantly in this case.
- The velocity field f' decreases for increasing values of Ha.
- In the presence of suction, the effect of an increase in Ha and β is to reduce the flow velocity and decrease the skin friction at the stretching surface, whereas the concentration increases with increase in β.
- Rate of mass transfer at the surface decreases with increase in M. Moreover, an increase in Sc decreases the concentration field ϕ.
- The concentration field ϕ decreases during destructive chemical reaction ($\gamma > 0$) and increases in generative chemical reaction ($\gamma < 0$).
- The study is useful in measurement and monitoring of viscosity, yield stress to control product quality in polymer solutions and melts, and the present study also contributed to the existing literature.

Acknowledgment

The authors are grateful to the reviewers for their comments and constructive suggestions.

References

[1] Sakiadis BC. Boundary-layer behavior on continuous solid surfaces. AIChE J 1961;7:26–8.
[2] Erickson LE, Fan LT, Fox VG. Heat and mass transfer on a moving continuous at plate with suction or injection. Ind Eng Chem Fundam 1966;5:19–25.
[3] Crane LJ. Flow past a stretching sheet. Z Appl Math Phys 1970;21:645–7.
[4] Gupta PS, Gupta AS. Heat and mass transfer on a stretching Sheet with suction or blowing. Can J Chem Eng 1977;55:744–6.
[5] Pavlov KB. Magnetohydrodynamic flow of an incompressible viscous fluid caused by deformation of a plane surface. Magnitnaya Gidrodinamika (U.S.S.R) 1974;4:146–7.
[6] Chakrabarti A, Gupta AS. Hydromagnetic flow and heat transfer over a stretching sheet. Q Appl Math 1979;37:73–8.
[7] Fetecau C, Fetecau C. The Rayleigh Stokes-problem for a fluid of Maxwellian type. Int J Non-Linear Mech 2003;38:603–7.
[8] Fetecau C, Fetecau C. An exact solution for the flow of a Maxwell fluid past an infinite plate. Int J Non-Linear Mech 2003;38:423–7.
[9] Sadeghy K, Sharifi M. Local similarity solution for the flow of a 'second-grade' viscoelastic fluid above a moving plate. Int J Nonlinear Mech 2004;39:1265–73.
[10] Liu IC. A note on heat and mass transfer for a hydromagnetic flow over a stretching sheet. Int Commun Heat Mass Transfer 2005;32:1075–84.
[11] Cortell R. Toward an understanding of the motion and mass transfer with chemically reactive species for two classes of viscoelastic fluid over a porous stretching sheet. Chem Eng Process: Process Intensification 2007;46:982–9.
[12] Andersson HI, Hansen OR, Holmedal B. Diffusion of a chemically reactive species from a stretching sheet. Int J Heat Mass Transfer 1994;37:659–64.
[13] Takhar HS, Chamkha AJ, Nath G. Flow and mass transfer on a stretching sheet with magnetic field and chemical reactive species. Int J Eng Sci 2000;38:1303–14.
[14] Akyilidiz FT, Bellout H, Vajravelu K. Diffusion of chemical reactive species in porous medium over a stretching sheet. J Math Anal Appl 2006;320:322–39.
[15] Layek GC, Mukhopadhyay S, Samad SA. Heat and mass transfer analysis for boundary layer stagnation-point flow towards a heated porous stretching sheet with heat absorption/generation and suction/blowing. Int Commun Heat Mass Transfer 2007;34:347–56.
[16] Hayat T, Awais M, Sajid M. Similar solutions of stretching flow with mass transfer. Int J Numer Meth Fluids 2010;64:908–21.
[17] Hayat T, Awais M, Qasim M, Hendi AA. Effects of mass transfer on the stagnation point flow of an upper-convected Maxwell (UCM) fluid. Int J Heat Mass Transfer 2011;54:3777–82.
[18] Pahlavan AA, Sadeghy K. On the use of homotopy analysis method for solving unsteady MHD flow of Maxwellian fluids above impulsively stretching sheets. Commun Nonlinear Sci Numer Simulat. 2009;14:1355–65.
[19] Hatami M, Mehdizadeh Ahangar GHR, Ganji DD. Electrohydrodynamic flow analysis in a circular cylindrical conduit using least square method. J Electrostatics 2014;72:47–52.
[20] Ghasemi SE, Hatami M, Ganji DD. Thermal analysis of convective fin with temperature-dependent thermal conductivity and heat generation. Case Stud Therm Eng 2014;4:1–8.
[21] Vatani M, Ghasemi SE, Ganji DD. Investigation of micropolar fluid flow between a porous disk and a nonporous disk using efficient computational technique. Proc Inst Mech Eng Part E: J Process Mech Eng 2014. http://dx.doi.org/10.1177/0954408914557375.
[22] Mohammadian E, Ghasemi SE, Poorgashti H, Hosseini M, Ganji DD. Thermal investigation of Cu–water nanofluid between two vertical planes. Proc IMechE Part E: J Process Mech Eng 2014. http://dx.doi.org/10.1177/0954408913509089.

[23] Khan WA, Culham JR, Makinde OD. Combined heat and mass transfer of third-grade nanofluids over a convectively-heated stretching permeable surface. Can J Chem Eng 2015;93:1880–8.
[24] Makinde OD. MHD mixed-convection interaction with thermal radiation and *n*th order chemical reaction past a vertical porous plate embedded in a porous medium. Chem Eng Commun 2011;198:590–608.
[25] Makinde OD, Sibanda P. Effects of chemical reaction on boundary layer flow past a vertical stretching surface in the presence of internal heat generation. Int J Numer Meth Heat Fluid Flow 2011;21:779–92.
[26] Makinde OD, Olanrewaju PO. Unsteady mixed convection with Soret and Dufour effects past a porous plate moving through a binary mixture of chemically reacting fluid. Chem Eng Commun 2011;198:920–38.
[27] Anwer Beg O, Makinde OD. Viscoelastic flow and species transfer in a Dacian high-permeable channel. J Petrol Sci Eng 2011;76:93–9.
[28] Jain MK, Iyengar SRK, Jain RK. Numerical methods for scientific and engineering computation. New Delhi, India: Wiley Eastern Ltd.; 1985.
[29] Prasad KV, Sujatha A, Vajravelu K, Pop I. MHD flow and heat transfer of a UCM fluid over a stretching surface with variable thermophysical properties. Meccanica 2012;47:1425–39.
[30] mukhopadhyay Swati, Golam Arif M, Wazed Ali PkM. Effects of transpiration on unsteady MHD flow of an UCM fluid passing through a stretching surface in the presence of a first order chemical reaction. Chin Phys B 2013;22:124701.
[31] Sharidan S, Mahmood T, Pop I. Similarity solutions for the unsteady boundary layer flow and heat transfer due to a stretching sheet. Int J Appl Mech Eng 2006;11:647–54.
[32] Chamkha AJ, Aly AM, Mansour MA. Similarity solution for unsteady heat and mass transfer from a stretching surface embedded in a porous medium with suction/injection and chemical reaction effects. Chem Eng Commun 2010;197:846–58.
[33] Bhattacharyya K, Mukhopadhyay S, Layek GC. Unsteady MHD boundary layer flow with diffusion and first order chemical reaction over a permeable stretching sheet with suction or blowing. Chem Eng Commun 2013;200:1–19.

Sudhagar Palani, M.SC, is a Ph.D student working under the supervision of Dr. Peri K Kameswaran and Dr. B Rushi Kumar at VIT University, Vellore, Tamil Nadu, India. Prior to beginning the Ph.D. program, he completed his M. Phill degree from Thiruvalluvar University, Vellore. His research interests include computational Fluid Dynamics, Heat and mass Transfer and boundary value problems. His dissertation focuses on Heat and mass Transfer problems on MHD boundary layer flows.

Dr. B. Rushi Kumar is presently working as an Associate Professor of Mathematics, Fluid Dynamics Division, School of Advanced Sciences, VIT University, Vellore, India. Dr. Rushi Kumar obtained his PhD degree in Mathematics in the area of Computational Fluid Dynamics (CFD) from Sri Venkateswara University, Tirupati, India. His research interests are Fluid Dynamics, Porous Media, Magnetohydrodynamics, Heat and Mass Transfer, Computational Fluid Dynamics, and Dr. Rushi Kumar has published 35 refereed research papers so far in various national, international journals and conferences. He has received research publications award from VIT University for his research publications.

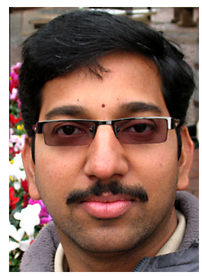

Peri K. Kameswaran is presently working as Assistant Professor Senior in Department of Mathematics, VIT University, Vellore. He is working on Numerical Studies on Mixed Convective Heat and Mass Transfer in Nanofluids. He completed Ph.D. in Andhra University, Visakhapatnam, Andhra Pradesh, India. During Ph.D., he worked several problems on Effects of Chemical reaction, double dispersion and Radiation on heat and mass transfer in non-Darcy fluid flows. He is interested in working on problems related to the Nanofluids and clear fluids by using numerical techniques. He is also a member of some mathematical societies. He presented a number of papers in various national and international conferences. He presented a paper in 2009, 2013 in ASME Conference, Florida, Sandiogo, USA. He did his Post Doctoral fellowship under the guidance of Precious Sibanda at the University of KwaZulu-Natal, South Africa.